STATISTICAL FLAW DETECTION IN A SCANNING MODE*

K.W. Fertig, J.M. Richardson, and R.K. Elsley

Rockwell International Science Center
1049 Camino Dos Rios
Thousand Oaks, California 91360

1. INTRODUCTION

The purpose of this paper is to describe an extension to an integrated model for assessing the performance of a given ultrasonic inspection system for detecting internal flaws. The integrated model is described in Fertig, Richardson, and Elsley (1984). The modified model incorporates the use of multiple waveform information obtained in a scanning mode. It is demonstrated that the proper use of this information can enhance the detectability of interior flaws. The next section describes the noise model for the scanning experiment. Section 3 develops an approximation to a decision theoretic solution to the detection problem and Section 4 provides a computer simulation.

2. NOISE MODEL

The original work of Fertig, Richardson, and Elsley (1984) referenced above considers a general pitch-catch transducer configuration. A computer code was written which simulates the ultrasonic measurement process. The transducer beam diffraction and refraction effects are modeled using the work of Thompson and Gray (1983,1984). Both flat and cylindrically curved interfaces are allowed for. The code has been modified so that in the scanning pulse-echo mode, time dependent waveforms can be recorded for discrete steps in the position of the transducer. This information can be displayed as "waterfall" plots as shown in Fig. 1. That figure shows the computer simulated ultrasonic response due to moving a transducer laterally over a slab of IN-100 with a planar interface. The noise process used in the figure is dominated by micropores within the IN-100.

---

*This work was sponsored by the Center for Advanced Nondestructive Evaluation, operated by the Ames Laboratory, USDOE, for the Air Force Wright Aeronautical Laboratories/Materials Laboratories under Contract No. W-7405-ENG-82 with Iowa State University.

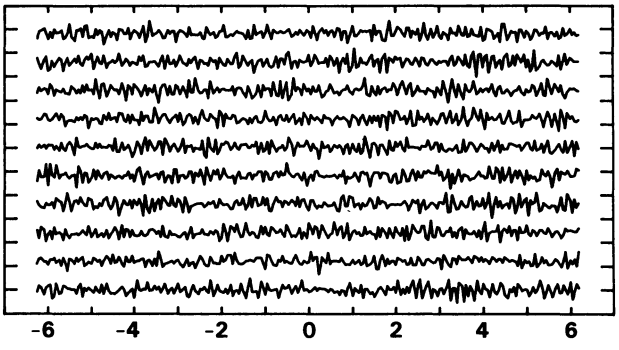

Fig. 1. Rainfall plot of time-dependent ultrasonic scans.

If we let $Y_\ell(t)$ represent the time dependent function for the ℓ^{th} position of the transducer, we seek to develop a relationship for the $\{Y_\ell\}$ in terms of various noise processes and internal localized scatterers that may be present. In order to account for the fact that the ultrasonic beams may overlap on different scan lines, we need a convenient model for describing the off-axis response of the transducer. To that end, we have assumed that the transducer behaves like a Gaussian transducer. The pressure field of a Gaussian transducer at a distance z from the wave is characterized by the complex parameter, q, given by

$$1/q(z) = 1/R(z) - 2i/k\omega^2(z) ,$$

where R(z) is the radius of curvature of the phase front, k is the wave number $(2\pi/\lambda)$, and $\omega(z)$ is the beam width (e.g., Yariv, A. (1971)). The off-axis pressure field is given by

$$p(x,y,z) = p(0,0,z)\exp[-x^2/s_x^2 - y^2/s_y^2] ,$$

$$s^2_{(x,y)} = -iq_{(x,y)}c/2\pi f ,$$

in which the subscripts x or y indicate that the beam can spread independently in each of these directions. See Thompson and Lopes (1984) for a more detailed description of Gaussian beams and their propagation through curved interfaces.

In the absence of a localized scatterer, the measured response $Y_\ell(\omega)$, in the frequency domain, of the ℓ^{th} scan is due to noise only. We include in our model additive electronic noise and additive material noise. Thus

$$Y_\ell(\omega) = \varepsilon_{mat_\ell}(\omega) + \varepsilon_{elec_\ell}(\omega) .$$

We may assume $\varepsilon_{elec_\ell}(\omega)$ is independent of $\varepsilon_{elec_m}(\omega)$ for $\ell \neq m$. This, however, is not the case for the material noise, since the beams for the ℓ^{th} and m^{th} scans may overlap. We show in Fig. 2 the situation for

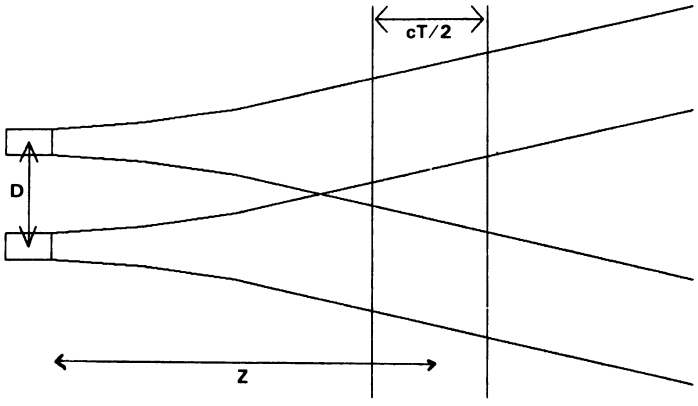

Fig. 2. Beam patterns for transducers a distance D apart.

transducers a distance D apart. Generally, the correlation between $Y_\ell(\omega)$ and $Y_m(\omega)$ will fall off as a function of D. In the Gaussian transducer case, if the material noise is due to a sea of randomly distributed scatterers in the material (e.g., grains, micro-pores, etc.), then in the Rayleigh limit,

$$\begin{aligned} \mathrm{var}(\varepsilon_{mat}) &= \omega^4 \langle |A_2|^2 \rangle Z |p(0)|^2 R_V/4 \\ &\cdot \pi |s_x^2||s_y^2| / [\mathrm{Real}(s_x^2)\mathrm{Real}(s_y^2)]^{\frac{1}{2}} , \end{aligned} \tag{1}$$

where A_2 is the low frequency scattering coefficient and $\langle |A_2|^2 \rangle$ means its expected square value taken over the distribution of localized scatterers, $|p(0)|^2$ is the amplitude squared of the on-axis system response function, R_V is the number of noise scatterers per unit volume, Z is the axial length of material sampled in the time windowed $Y_\ell(t)$ ($Z = c_1 T/2$, T = time window), ω is temporal frequency, and s_x^2 and s_y^2 are the Gaussian beam variances. This equation comes from the following more basic formulation.

Consider real space partitioned into cells of size $\delta x \delta y \delta z$ with the k^{th} cell having center (x_k, y_k, z_k). Consider each noise contributing scatterer having an internal state (e.g., size and orientation) parameter, s. If we partition the scatterer state space into "cells" of size δs with centers s_m, and let ν_{mk} be the number of scatterers with state in the m^{th} state cell and having centers in the k^{th} space cell, then we can write the measured material noise $\varepsilon_{mat_\ell}(\omega)$ for the ℓ^{th} waveform as

$$\begin{aligned} \varepsilon_{mat_\ell}(\omega_j) &= \sum_k \sum_m \nu_{mk} A(\omega_j, s_m) p_0(\omega_j) \\ &\cdot \exp\left[-(x_k - x_\ell)^2 / s_{x_{j\ell}}^2 - (y_k - y_\ell)^2 / s_{y_{j\ell}}^2 \right] \\ &\cdot \exp[-2i\omega/c_1 (z_k - z_{1\ell})] , \end{aligned} \tag{2}$$

where $z_{1\ell}$ is the position in the material corresponding to the center of time for the ℓ^{th} scan, $A(\omega_j,s_m)$ is the far-field scattering amplitude for a scatterer of state s_m, $p_0(\omega_j)$ is the on-axis system response function for the ℓ^{th} scan (centered at $z_{1\ell}$ and assumed independent of ℓ for simplicity), k_1 is the wave number in the material, and $s^2_{x_{j\ell}}$ and $s^2_{y_{j\ell}}$ are the Gaussian beam parameters for the j^{th} frequency, ω_j, and the ℓ^{th} scan. Formula (2) assumes no multiple scattering.

We can choose $\delta x\delta y\delta z\delta s$ so small that $P[\nu_{mk} > 1] \simeq 0$ where $P[E]$ means the probability that event E occurs. We let $N(s)$ be the density of scatterers in the sense that $\langle\nu_{mk}\rangle = N(s_m)\delta x\delta y\delta z\delta s$, where $\langle\bullet\rangle$ means expectation. If we take the expectation of (2) with respect to the ν_{mk} and let the cell size go to zero, the summations go over into integrals and we obtain

$$\langle\varepsilon_{mat_\ell}(\omega_j)\rangle = 0$$

for $\omega_j = j\Delta\omega$, $\Delta\omega = 2\pi/T$, where T is the time window. We get equation (1) for $\langle\varepsilon_{mat}\varepsilon^*_{mat}\rangle \equiv var(\varepsilon_{mat})$.

From equation (2), we can compute the covariance between ε_{mat_ℓ} and ε_{mat_m}. In the case of a planar interface, with possibly non-normal incidence, we obtain

$$cov(\varepsilon_{mat_\ell}(\omega_j),\varepsilon_{mat_m}(\omega_{j'})) = \delta_{jj'}var(\varepsilon_{mat})exp[-D^2/2Re(s_x^2)] ,$$

where D is the distance between the transducers in the i^{th} and m^{th} scans.

For normal incidence, planar interface, $Re(s_x^2) = a^2/2$, where a is the radius of the transducer. Thus, we see the correlation between waveforms is $exp[-D^2/a^2]$. This falls off very rapidly with respect to transducer distance D and is independent of frequency and depth.

Combining the electronic noise into the model, we have

$$\begin{aligned} cov(Y_{\ell j},Y_{mj}) &\equiv C_{\ell jmj} \\ &= var(\varepsilon_{mat})exp[-(\ell - m)^2D_0^2/2Re(s_x^2)] \\ &\quad + \delta_{\ell m}var(\varepsilon_{elec}) \end{aligned} \tag{3}$$

where D_0 is the step between adjacent transducer scans. The reader is cautioned that this formula is valid for parallel beams only and hence requires planar interfaces with transverse scans.

3.0 DETECTION ALGORITHM

The detection of an isolated flaw can be performed using an algorithm based on decision theoretic considerations. Following last year's work (Fertig, Richardson, and Elsley (1984)), we take as a flaw model, a generalized scatterer represented by a sum of δ-functions. If we scale the scatterer "size" by a parameter θ, we take as our measurement model,

$$Y_\ell(\omega_j) = p_0(\omega_j)\theta A(\omega_j)\exp[-(x_f - x_\ell)^2/s_x^2 - (y_f - y_\ell)^2/s_y^2]$$
$$\cdot \exp[-2i\omega z_f/c_1] + \varepsilon$$

where p_0 is the on-axis system response function, (x_f,y_f,z_f) is the flaw position, s_x^2 and s_y^2 are the Gaussian beam parameters, and $A(\omega_j)$ is the far-field scattering amplitude associated with a beam whose center axis is incident on the scatterer. Note, we have ignored the angular effect on $A(\omega)$ for off-axis beams by not considering it a function of flaw position relative to an off-axis beam position. It would be an easy matter to correct for this effect.

The detection problem reduces to testing the hypothesis $H_0 : \theta = 0$ versus $H_A : \theta \neq 0$. As was done in Fertig, Richardson, and Elsley (1984), we use the maximum likelihood ratio statistic,

$$\lambda = \frac{\sup_{H_A \cup H_0} \text{Lik}(\{Y_\ell\}|\theta,x_f,y_f,z_f)}{\sup_{H_0} \text{Lik}(\{Y_\ell\}|\theta,x_f,y_f,z_f)} . \tag{4}$$

In order to carry out the process, we need the joint probability of all the $Y_\ell(\omega_j)$. This is a simple matter to write down if we assume that the noise is Gaussian with moments given in Section 2.0. The maximization in the denominator of (4), in which we are constrained by H_0, is trivial since there is only one likelihood function when $\theta = 0$. The maximization in the numerator involves maximizing with respect to θ for each assumed flaw position x_f,y_f,z_f and then maximizing with respect to this position.

Maximization with respect to θ can proceed analytically. If we assume the flaw is on the axis of a scan, say scan $(L + 1)/2$, then

$$\ell n\ \lambda \propto \sup_k \text{Real} \left\{ \sum_{\ell=1}^{L} \sum_{j=1}^{J} Y_{\ell j} G_{\ell j} \exp[2i\omega_j z_k/c_1] \right\} \tag{5}$$

where

$$G_{\ell j} = \sum_m C^{\ell j m j} p_j^* \exp[-(m - \ell)^2 D_0^2/s_x^{2*}] ,$$

and p_j is the on-axis system response function at frequency ω_j, D_0 is the transducer spacing between adjacent scans, s_x^2 is the complex Gaussian beam variance, and $C^{\ell jmj}$ is the inverse of the variance-covariance matrix, $C_{\ell jmj}$, given by equation (3). We have assumed scanning is in the x-direction.

Operationally, we see that this is a simple filtering process. The weights $G_{\ell j}$ are computed and stored off line. Given the data $Y_{\ell j}$, we form the waveform $\hat{Y}_j = \sum_{\ell=1}^{L} G_{\ell j} Y_{\ell j}$. This waveform is then fast-Fourier transformed according to (5) to yield the real time dependent waveform $\overline{Y}_k = \sum_j \hat{Y}_j \exp[2\pi ikj]$.

The hypothesis H_0 is rejected, i.e., we decide there is a flaw present, if $\ell n\ \lambda$ is greater than some threshold. Equivalently, we can threshold the time dependent waveform $\overline{Y}_k$ to make the detection decision.

4. COMPUTER SIMULATION EXAMPLE

Consider the inspection of a slab of IN-100 at normal incidence with a 5 MHz transducer using longitudinal waves. For a 5 cm waterpath, and 1.27 cm material path, the on-axis system response function corrected for diffraction is shown in Fig. 3. We use a noise model with 1)

$$\mathrm{var}(\varepsilon_{mat}) = [3.22 \times 10^{-6}\,\mathrm{cm}^{-1}(\mathrm{rad}/\mu\mathrm{sec})^{-2}]^2\omega^4 V(\omega) \ ,$$

where $V(\omega) = \pi a^2(c_1 T/2)(1 + (\lambda_0 z_0 + \lambda_1 z_1)/\pi a^2)$, in which T is the window time (12 μsec), z_0 and z_1 are the water and material path lengths, and a is transducer radius (.3175 cm), and with 2)

$$\mathrm{var}(\varepsilon_{elec}) = 0.01 \ .$$

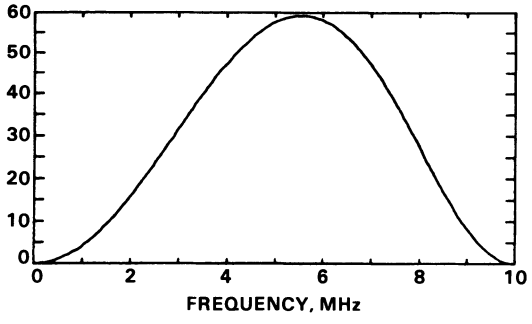

Fig. 3. On-axis system response function for nominal 5 MHz, ½ inch diameter transducer. Transducer beam is normal to a water/IN-100 interface. The waterpath is 5 cm; the IN-100 path is 1.27 cm.

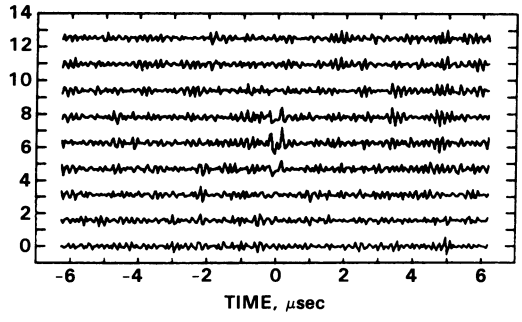

Fig. 4. Scattering off of 500 μ radius circular crack with normal 70° to the beam axis. This is for nine scan positions ¼ inch apart. Transducer used is described in Fig. 3. Flaw is centered on fifth scan line.

This noise model is matched to an IN-100 specimen investigated by Titt-mann and Ahlberg (1983).

Assume there is a 500 μ crack with a normal 70° off of the z-axis which is taken parallel to the transducer beam. The raw time dependent data for scans one transducer radius apart are shown in Fig. 4. The scattering due to the flaw has been added using the Kirchoff approximation and shows up in the center of the figure.

If these data are processed one waveform at a time (L = 1 in Section 3), the appropriate filter is shown in Fig. 5. When this filter is applied to each of the waveforms in Fig. 4 one waveform at a time, the result is shown in Fig. 6. It can be seen that essentially all the noise is suppressed and the flaw shows up in increasing amplitude towards the center of this figure. The improvement over video detection is dramatic.

If the data in Fig. 4 are processed five waveforms at a time (L = 5 in Section 3), we use the filters shown in Fig. 7. Again, these are low pass filters. There is a small phase variation for the waveforms that

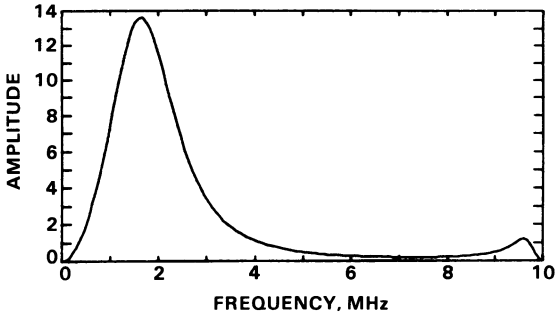

Fig. 5. Real time filter for 5 MHz transducer described in Fig. 3 and noise model described in text.

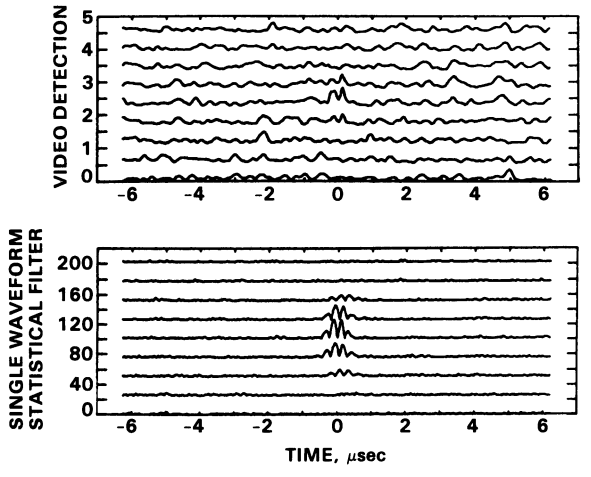

Fig. 6. Output of video detection (envelope thresholding) and statistical filtering when the data in Fig. 4 are viewed one waveform at a time.

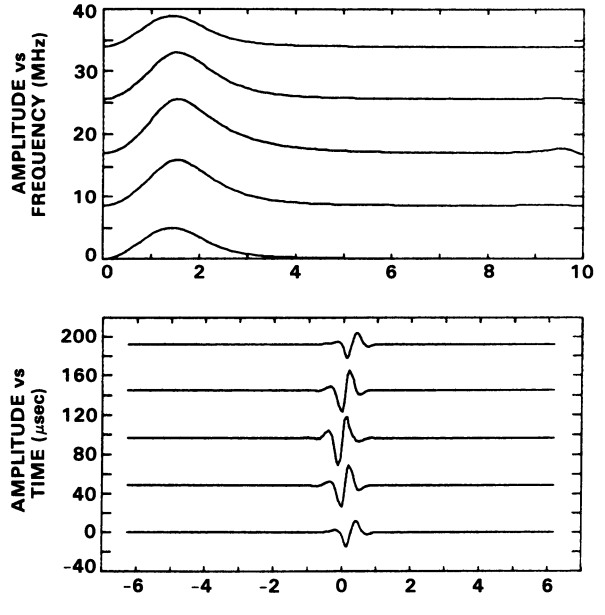

Fig. 7. Statistical filters $(G_\ell(\omega_j)\ell = 1,\cdots,5)$ for processing raw scan data with a moving window of five waveforms at a time.

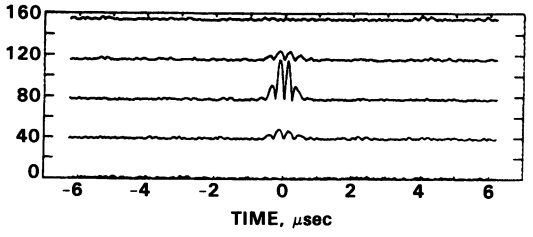

Fig. 8. Output of statistical filtering of the data in Fig. 4. The bottom waveform is the result of combining $Y_1,\cdots,Y_5$ in Fig. 4. The second to bottom waveform is the result of combining $Y_2,\cdots,Y_6$. The middle waveform is the result of combining $Y_3,\cdots,Y_7$, etc.

are assumed off the axis of the flaw. This is as it should be since the travel time from the flaw to the transducer increases slightly as the flaw moves off axis. If these filters are applied to the data in Fig. 4 in groups of five waveforms at a time (i.e., first apply the filters to $Y_1,\cdots,Y_5$, then to $Y_2,\cdots,Y_6,\cdots$, then to $Y_5,\cdots,Y_9$), the result is Fig. 8. It can be seen that the flaw stands out even clearer. It is apparent that some of the energy spilling over into adjacent waveforms in the one-at-a-time approach typified by Fig. 6 is being concentrated into the center waveform in Fig. 8. From this and similar experiments we have concluded that the decision theoretic based algorithm employing scanning information improves detectability over the one-waveform-at-a-time decision theoretic based algorithm, which in turn is a dramatic improvement over the more usual video detection algorithm.

REFERENCES

Fertig, K.W., J.M. Richardson, and R.K. Elsley (1984), "Statistical Flaw Detection: Theory," Review of Progress in Quantitative Nondestructive Evaluation, D.O. Thompson and D.E. Chimenti, Editors, Plenum Press, Vol. 3A, pp. 65-80.

Thompson, R.B. and T.A. Gray (1983), "Analytical Diffraction Corrections in Ultrasonic Scattering Measurements," Review of Progress in Quantitative Nondestructive Evaluation, Vol. 2A, pp. 567-586.

Thompson, R.B. and T.A. Gray (1984), "Application of Diffraction Corrections to the Absolute Measurement of Scattering Amplitudes," Review of Progress in Quantitative Nondestructive Evaluation, Vol. 3A, pp. 373-383.

Yariv, A. (1971), Introduction to Optical Electronics, Holt, Rinehart and Winston, Inc., New York.

Thompson, R.B. and E.F. Lopes (1984), "The Effects of Focusing and Refraction on Gaussian Ultrasonic Beams," this Proceedings.

Tittmann, B.R. and L.A. Ahlberg (1983), "Attenuation and Grain Noise Parameters in Ni-Base Alloys," Review of Progress in Quantitative Nondestructive Evaluation, Vol. 2A, pp. 129-145.